Formation of a High T_c Electron-Hole Liquid in Diamond

Ryo Shimano,[1] Masaya Nagai,[1] Kenji Horiuch,[2] and Makoto Kuwata-Gonokami[1,*]

[1]*Department of Applied Physics, the University of Tokyo, and Cooperative Excitation Project ERATO, Japan Science and Technology Corporation (JST), 7-3-1, Hongo, Bunkyo-ku, Tokyo 113-8656 Japan*

[2]*Frontier Laboratory, R&D Planning Department, Tokyo Gas Company, Ltd., 1-7-7, Suehiro-cho, Tsurumi-ku, Yokohama, 230-0045 Japan*

(Received 27 July 2001; published 18 January 2002)

We report on the observation of electron-hole (*e-h*) liquid (EHL) in diamond by time-resolved luminescence measurements under an intense femtosecond photoexcitation above the band gap. The EHL luminescence band is observed below the *e-h* plasma band, showing a finite rise time of several tens of picoseconds. The rise time, which corresponds to the nucleation and the growth of the *e-h* droplets, plummets on approaching the EHL critical temperature. Time-resolved spectral shape analysis reveals a very high carrier density of 1×10^{20} cm^{-3} and very high critical temperature of $T_c = 165$ K of EHL.

DOI: 10.1103/PhysRevLett.88.057404 PACS numbers: 78.47.+p, 71.30.+h, 71.35.Ee, 71.35.Lk

At high excitation density, the photogenerated electrons and holes in semiconductors constitute a unique playground to study the system of charged particles driven by the Coulomb correlation. For several decades, attention here has been focused on low-temperature phases and, especially, on the dense electron-hole (*e-h*) liquid (EHL), the physical properties of which are similar to those of liquefied metals [1]. EHL has been observed in Ge, Si [2], GaP [3], SiC [4], and AlGaAs [5]. In these indirect-gap semiconductors, the density of photogenerated carriers can be varied within a wide range, allowing one to obtain the quasiequilibrium phase diagram. In particular, the interplay of the metal-insulator and liquid-gas phase transitions that has been discussed for the first time for mercury [6] has recently attracted a lot of interest [7]. The study of the underlying mechanisms of phase transitions in this system has recently become possible by using a novel ultrafast laser technique. However, the usually very low critical temperature (T_c) of the EHL in indirect-gap semiconductors (see Table I) brings severe limitation on the systematic study. This is partially due to a large dielectric constant, which screens the *e-h* correlation and raises the EHL ground-state energy. In this paper we show that diamond is a high T_c material which enables the study of the dynamics of the photogenerated carriers with high quantum degeneracy in a wide range of temperature and density.

Diamond, an indirect-gap semiconductor with large band gap energy, is a good candidate to show a stable EHL phase and high T_c. The reason is twofold. First, the dielectric constant of diamond is much smaller than that in other indirect-gap semiconductors (see Table I). This reduces the Coulomb screening and increases the T_c of EHL. Second, diamond has the sixfold degenerate conduction band minimum $\mathbf{k}^c_{\min}$ along [100] axes at 76% of the X point and a twofold degenerate valence band extremum at $\mathbf{k} = 0$. In addition, the spin-orbit splitting of the valence band between Γ_7 and Γ_8 [8] is very small (6 meV). Similar degeneracy of the band structure in Ge and Si [1] reduces the kinetic energy and stabilizes the EHL phase. Calculations predict the formation of EHL droplets in diamond at a density of 10^{20} cm^{-3} and relatively high (above 100 K) temperature [9], while the recent steady-state photoluminescence measurements [10] may suggest creation of EHL droplets. However, such high density enhances the nonradiative Auger recombination, making the EHL lifetime in diamond shorter in comparison with that in Ge and Si [11] and making interpretation of the luminescence spectra and, in particular, separation of the EHL and excitonic luminescence in steady-state measurements difficult. Recent advances in the technology of single crystal growth and ultraviolet femtosecond light sources have made it possible to study the intrinsic dynamics of a high density *e-h* system.

In order to clarify the formation of the quasiequilibrium EHL, we perform time-resolved photoluminescence measurements, which enable us to overcome the limitations of the steady-state experiment and temporally resolve the exciton, EHL, and *e-h* plasma (EHP) luminescence in diamond. We clearly observe the finite rise time of the EHL luminescence and reveal its sharp decrease at $T = 135$ K. This enables us to confirm very high T_c of EHL in diamond.

We use a sample grown by the high-temperature and high-pressure method with the size of $2 \times 2 \times 0.5$ mm [12]. The fourth harmonic of a regenerative amplified

TABLE I. Values of band gap energy, dielectric constant, density of EHL at $T = 0$, critical temperature, and decay constant in various indirect-gap semiconductors. The above parameters for Ge and Si are from Ref. [1], those for GaP are from Ref. [3], those for SiC are from Ref. [4], and those for diamond are from this paper.

	E_g (eV)	ϵ_b	n_0 (cm^{-3})	T_c (K)	τ_0
Ge	0.74	16.0	2.5×10^{17}	6.7	40 μs
Si	1.16	12	3.3×10^{18}	24.5	150 ns
GaP	2.35	9.1	6×10^{18}	40	35 ns
3C-SiC	2.39	9.72	7.8×10^{18}	41	57 ns
Diamond	5.49	5.7	1.0×10^{20}	165	0.8 ns

 © 2002 The American Physical Society

mode-locked Ti:sapphire laser set to 808 nm (0.2 ps pulse duration and 1 kHz repetition rate) is used as an excitation light source with the photon energy of 6.1 eV, which is above the indirect-gap of diamond. The excitation pulse at 202 nm is generated via the sum frequency generation process in a β-BBO crystal, which is irradiated by the fundamental pulse and its third harmonic. The excitation pulse is focused on a sample with a spot size of 70 μm. The sample is kept in a closed cycled cryostat, and the temperature is varied from 15 K to room temperature. The luminescence is measured using a spectrometer with a focal length of 27 cm equipped with a cooled backilluminated CCD camera. For the time-resolved luminescence measurement, a 50 cm spectrometer equipped with a streak camera (Hamamatsu M1955) is used. The temporal and spectral resolutions are 25 ps and 0.3 nm, respectively.

Figure 1 shows the time-integrated luminescence spectra at 15 K (a) and 293 K (b) and excitation densities from 0.03 mJ/cm^2 to 23 mJ/cm^2. One can observe that a narrow TO phonon-assisted free-exciton line at 5.27 eV [13,14] dominates the luminescence at 15 K. The absence of the bound exciton luminescence [13,14] even at low temperature and low excitation density indicates the high purity of the sample. At high excitation density, new luminescence bands appear at 5.16 and 5.02 eV, which line shapes are broad and symmetric. Relatively weak free-exciton lines assisted by the TA, LO, and TO + optical phonon at $\mathbf{k} = 0$ are also observed at 5.32, 5.24, and 5.11 eV, respectively. The exciton luminescence persists even at 293 K [Fig. 1(b)] due to the large exciton binding energy of 80 meV [8,13]. When the excitation density is increased, the luminescence at the lower-energy side becomes pronounced. We examine the temperature dependence of the luminescence spectra under the strong excitation level of 23 mJ/cm^2 by changing the lattice temperature from 15 to 293 K. As the temperature increases, the broadband luminescence centered at 5.16 eV becomes weaker and shows a small blueshift. Above 130 K, it merges to an exciton luminescence line as a broad asymmetric sideband.

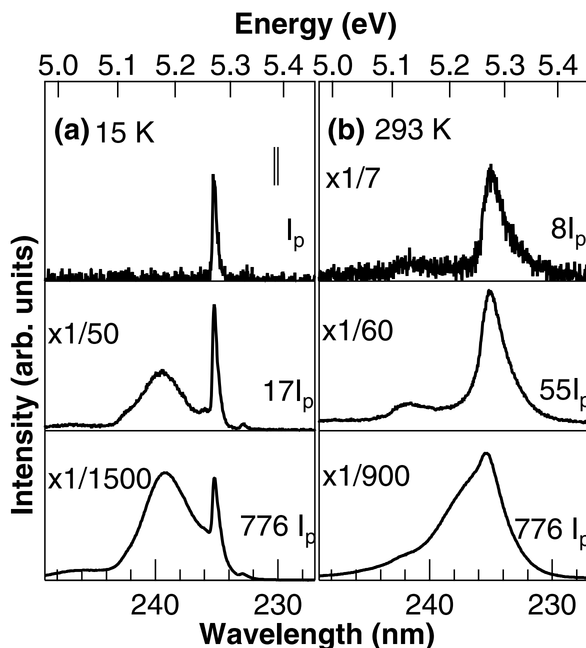

FIG. 1. Time-integrated luminescence spectra at 15 K (a) and 293 K (b) using 202 nm femtosecond pulse excitation. The excitation density is $I_p = 0.03$ mJ/cm^2. The spectral resolution is shown in (a).

The luminescence spectrum of Si has been found to show similar temperature dependence [15]. Specifically, the broad and symmetric band observed at $T < T_c$ ($T_c =$ 23 K) can be assigned to EHL, while the asymmetric luminescence band observed at $T > T_c$ can be assigned to the EHP. The coexistence of EHL, EHP, and excitons, however, makes the analysis of the time-integrated spectra rather difficult, even for Ge and Si [7].

Figure 2 shows time-resolved luminescence spectra at 0.1, 0.7, and 1.7 ns after excitation at temperatures of 15 K (a) and 290 K (b) and excitation density of 13 mJ/cm^2. At 15 K, broadband luminescence at 5.18 eV dominates at 100 ps after the excitation. Total luminescence intensity decays with time, while the central frequency and spectral shape remain almost the same (a small redshift, which is observed between 0.1 and 0.7 ns, will be discussed later). As soon as the excitation density exceeds the broadband luminescence threshold, the temporal evolution of the luminescence becomes independent on the excitation density. At 290 K, broadband luminescence with a maximum at 5.23 eV appears at 0.1 ns after the excitation. In contrast to the case of 15 K, we observed a gradual blueshift of the maximum with time. The shift reaches 5.28 eV at

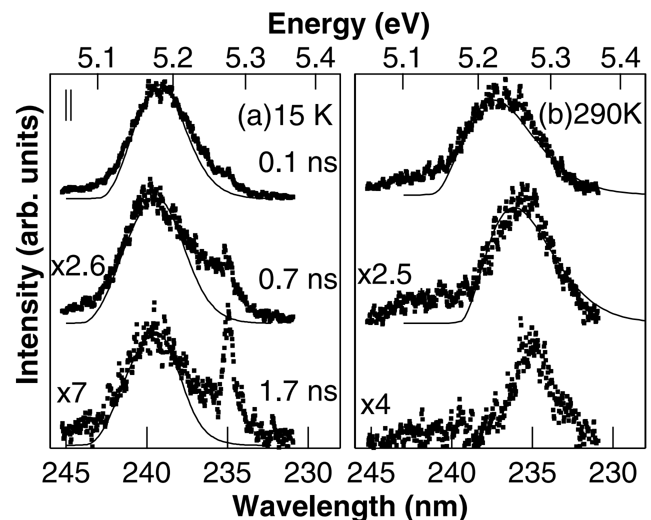

FIG. 2. Time-resolved luminescence spectra at an excitation density of 13 mJ/cm^2 at 0.1, 0.7, and 1.7 ns after the excitation and temperature of (a) 15 K and (b) 290 K. The intensity is normalized. The solid lines show the fitting curve with Fermi-liquid line shape analysis.

1.7 ns and is accompanied by the continuous narrowing of the bandwidth.

The luminescence line shape of EHL and EHP is given by the the Fermi distributions of electron and hole, densities of states, assisted phonon energies, and renormalized band gap energy, E_g' [7]. The reduction of the band gap energy at finite excitation density ("band gap renormalization") can be described as $E_g' = E_g(T_L) + \partial(nE_{xc})/\partial n$. Here $E_g(T_L)$ is the band gap energy at lattice temperature T_L, n is the carrier density, and E_{xc} is the sum of the Coulombic exchange and correlation energies [16]. It has been shown [17] that E_{xc} can be approximated by a simple form in terms of the exciton Rydberg energy E_R and $r_s = (3/4\pi n a_B)^{1/3}$, where a_B is the exciton Bohr radius.

We determine E_g' from the position of the lower-energy edge of the EHP or EHL luminescence bands. By fitting the time-resolved luminescence spectra with the Fermi-liquid line shape [7], as shown by solid lines in Fig. 2, we can obtain temporal evolution of the carrier density n and temperature T_{eff}, along with the luminescence intensity proportional factor I_0. We account for the valley multiplicity by weighting the effective masses of electrons and holes to $1.7m_e$ and $0.87m_e$, respectively [13]. The spectra are dominated by TO phonon-assisted emission, while contributions from the TA- and LO-phonon processes are considerably smaller. In our analysis, the relative contributions of these phonon-assisted bands were estimated from the free-exciton luminescence spectra as the following: $I_0^{\mathrm{TA}}/I_0^{\mathrm{TO}} = I_0^{\mathrm{LO}}/I_0^{\mathrm{TO}} = 0.05$.

Figure 3 shows the obtained temporal evolution of the carrier density at different temperatures and excitation density. At $T = 290$ K and excitation of 107 mJ/cm^2, the initial carrier density is estimated as 1×10^{20} cm^{-3} and decreases with time [open squares (a)]. At a lower excitation of 13 mJ/cm^2, the carrier density starts from 3×10^{19} cm^{-3} and decreases with time [closed circles (b)]. This result is consistent with the gradual blueshift of the luminescence peak in Fig. 2(b), which indicates the recovery of band gap shrinkage with decreasing carrier density. On the contrary, at $T = 15$ K, the carrier density remains constant, i.e., $n = 1.0 \times 10^{20}$ cm^{-3} up to 2 ns at an excitation density of 13 mJ/cm^2 [open circles (c)]. Similar temporal evolution is also obtained for the lower excitation density of 4 mJ/cm^2 [close squares (d)], clearly indicating the formation of EHL in diamond.

Time-resolved measurements allow us to examine the formation dynamics of the EHL phase. Figure 4 shows the temporal evolution of luminescence intensity for the high-energy side (**A**) and low-energy side (**B**) of the band at the excitation density of 4 mJ/cm^2, which is just above the threshold of the EHL or EHP luminescence. At $T = 15$ K, there is a 60 ps rise time of the luminescence intensity at the lower-energy side of the band, while the intensity at the high-energy side rises within our temporal resolution. This indicates that luminescence spectra shift towards the low-energy side during the buildup time of the EHL. Figure 4(c) shows that no pronounced delay is observed at $T = 146$ K. This suggests that the finite rise time of the EHL luminescence on Fig. 4(a) corresponds to the nucleation and the growth time of the EHL droplets. In our experimental condition, the photoexcitation results in the creation of e-h pairs (i.e., free excitons or a low density plasma) within the pulse duration. The carriers reduce their effective temperature and transform themselves into e-h clusters, which eventually grow into macroscopic e-h droplets within several tens of picoseconds. Thus, the luminescence at the low-energy side, which is characteristic of the EHL, rises gradually within a finite time necessary for nucleation.

On approaching the EHL critical temperature, the nucleation time decreases and finally plummets at T_c because

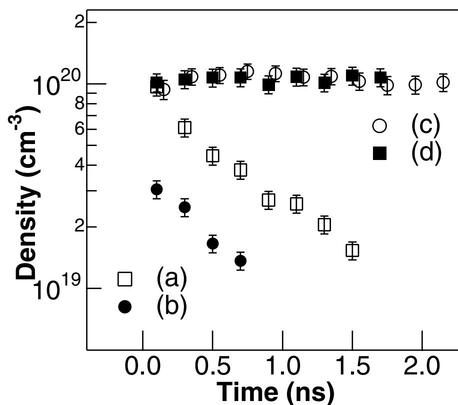

FIG. 3. Temporal evolution of carrier density n estimated from the line shape analysis of phonon-assisted emission at 290 K with excitation density (a) 107 mJ/cm^2 (open squares) and (b) 13 mJ/cm^2 (closed circles) and at 15 K with excitation density (c) 13 mJ/cm^2 (open circles) and (d) 4 mJ/cm^2 (closed squares). Phonon dispersion is neglected in this analysis.

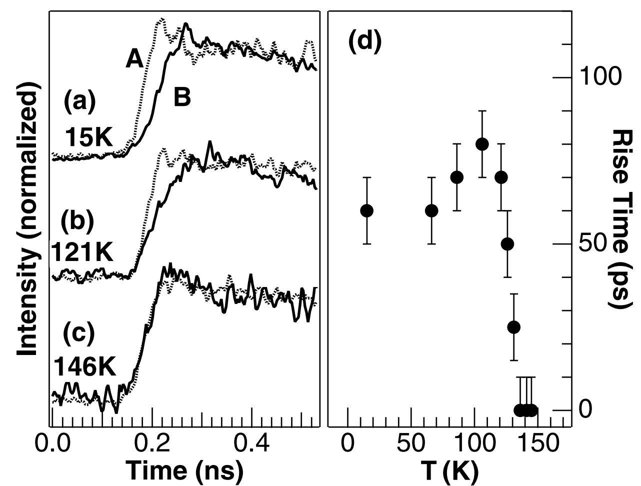

FIG. 4. Temporal evolution of luminescence intensity at 5.23 eV (**A**: dotted line) and 5.15 eV (**B**: solid line) and at (a) 15 K, (b) 121 K, and (c) 146 K. (d) The temperature dependence of luminescence rise time. The length of the error bars denotes a temporal resolution of the streak camera.

the nucleation in supercooled gas is triggered by statistical fluctuation [18]. Our temperature dependence measurements show that the luminescence rise time drops at a temperature of $T = 135$ K [see Fig. 4(d)]. The analysis of the luminescence spectra gives the corresponding critical carrier temperature, which we find to be equal to $T_c = 165$ K. The higher-energy edge of the luminescence band gives the total energy of the e-h pair measured from the band gap (i.e., the ground-state energy of EHL) as $E_0 = -0.13$ eV (the EHL work function of 0.05 eV, with respect to the exciton with the binding energy of 80 meV). The ratio $|E_0|/k_B T_c = 9.3$ in diamond is found to be reasonably close to 10.3 ± 0.7 in Ge, 11.7 ± 1.7 in Si, 9.5 in GaP, and 11 in SiC [2–4]. This agrees well with the result of the numerical simulation, which predicts that $|E_0|/k_B T_c$ is almost constant for various band structures [19].

One can observe from Fig. 2 that the EHL luminescence shows a rather fast decay time of the order of 1 ns. A single exponential decay fitting returns the decay lifetime of $\tau = 1.0$ ns at 15 K, which is much faster than an exciton lifetime [20]. This implies that there exists an efficient nonradiative decay mechanism that dominates and shortens the EHL lifetime. In Ge and Si, it is known that the Auger recombination determines the lifetime of EHL. The Auger recombination rate is proportional to the square of the e-h pair density n, $1/\tau = Cn^2$, where the coefficient C has been found to be 3×10^{-31} and 7.5×10^{-31} cm^6/s for Ge and Si [21]. This is also consistent with theoretical estimations [22,23]. If we assume that the observed decay time in diamond is also dominated by the Auger recombination, we arrive at $C = 1 \times 10^{-31}$ cm^6/s, which is almost similar to those in other indirect-gap materials. Therefore, we can conclude that the Auger recombination is an efficient decay mechanism in the EHL of diamond.

In summary, we report on the observation of EHL under strong photoexcitation above the band gap energy in diamond. Time-resolved luminescence measurements clearly show the existence of a liquid phase and a nucleation process to form droplets. The critical EHL temperature in diamond is 165 K, which is much higher than that of Ge and Si. The fast decay of EHL emission (1.0 ns), is attributed to the nonradiative Auger recombination process. The observed nucleation time is several tens of picoseconds, which is comparable to the formation time of EHL droplets recently observed in a direct-gap semiconductor [24]. Further experiments on the formation dynamics of EHL droplets will bring new insights on the nonequilibrium quantum kinetics, which has been intensively studied for several decades [25].

We thank K. Nakamura and S. Yamashita for providing a high-quality synthetic diamond crystal and for their helpful discussions, and we are also grateful to Yu. P. Svirko for fruitful discussions.

---

*Author to whom correspondence should be addressed. Email address: gonokami@ap.t.u-tokyo.ac.jp

[1] *Electron-Hole Droplets in Semiconductors,* edited by C. D. Jeffries and L. V. Keldysh (North-Holland, Amsterdam, 1983).
[2] See, e.g., J. C. Hensel, T. G. Phillips, and G. A. Thomas, in *Solid State Physics,* edited by H. Ehrenreich, F. Seitz, and D. Turnbull (Academic, New York, 1977), Vol. 32, and references therein.
[3] J. Shah, R. F. Leheny, W. R. Harding, and D. R. Wight, Phys. Rev. Lett. **38**, 1164 (1977).
[4] D. Bimberg, M. S. Skolnick, and W. J. Choyke, Phys. Rev. Lett. **40**, 56 (1978).
[5] H. Kalt, K. Reimann, W. W. Rühle, M. Rinker, and E. Bauser, Phys. Rev. B **42**, 7058 (1990).
[6] L. D. Landau and Y. B. Zeldovich, Acta Phys. Chem. USSR **18**, 194 (1943).
[7] L. M. Smith and J. P. Wolfe, Phys. Rev. B **51**, 7521 (1995).
[8] *Properties and Growth of Diamond,* edited by G. Davies (Institution of Electrical Engineers, London, 1994).
[9] M. A. Vouk, J. Phys. C **12**, 2305 (1979).
[10] K. Thonke *et al.,* Diam. Relat. Mater. **9**, 428 (2000).
[11] It is found that the Auger recombination rate τ_0 obeys the relation, $\tau_0/n_0^2 = \mathrm{const}$, with density n_0; see R. M. Westervelt, in *Electron-Hole Droplets in Semiconductors* (Ref. [1]), Chap. 3, p. 252. This relation gives a short lifetime of less than 1 ns of e-h droplets in diamond.
[12] K. Horiuchi, K. Nakamura, S. Yamashita, and M. Kuwata-Gonokami, Jpn. J. Appl. Phys. **36**, 1505 (1997).
[13] P. J. Dean, E. C. Lightowlers, and D. R. Wight, Phys. Rev. **140**, A352 (1965).
[14] A. T. Collins, S. C. Lawson, G. Davies, and H. Kanda, Phys. Rev. Lett. **65**, 891 (1990).
[15] J. Shah, M. Combescot, and A. H. Dayem, Phys. Rev. Lett. **38**, 1497 (1977).
[16] E. A. Andryushin *et al.,* JETP Lett. **24**, 185 (1976).
[17] P. Vashishta and R. K. Kalia, Phys. Rev. B **25**, 6492 (1982).
[18] L. D. Landau and E. M. Lifshitz, *Statistical Physics* (Pergamon, Oxford, 1959).
[19] T. L. Reinecke and S. C. Ying, Phys. Rev. Lett. **43**, 1054 (1979); **43**, 1627(E) (1979).
[20] K. Takiyama, M. I. Abd-Elrahman, T. Fujita, and T. Oda, Solid State Commun. **99**, 793 (1996).
[21] C. Benoit à la Guillaume, M. Voos, and Y. Pétroff, Phys. Rev. B **10**, 4995 (1974).
[22] A. Haug, Solid State Commun. **25**, 477 (1977).
[23] D. Hill and P. T. Landsberg, Proc. R. Soc. London A **347**, 547 (1976).
[24] M. Nagai, R. Shimano, and M. Kuwata-Gonokami, Phys. Rev. Lett. **86**, 5795 (2001).
[25] H. Haug and F. F. Abraham, Phys. Rev. B **23**, 2960 (1981).